AMSI VACATION RESEARCH SCHOLARSHIPS 2019–20

EXPLORE THE MATHEMATICAL SCIENCES THIS SUMMER

The Rarefied Gas Dynamics of Levitating Microdisks

Matthew Walker

Supervised by Prof. John Sader & Dr Jesse Collis

ARC Centre of Excellence in Exciton Science

School of Mathematics & Statistics

The University of Melbourne

Vacation Research Scholarships are funded jointly by the Department of Education and Training and the Australian Mathematical Sciences Institute.

AMSI AUSTRALIAN MATHEMATICAL SCIENCES INSTITUTE

Australian Government Department of Education

Contents

Abstract

In a recent experiment, the levitation of macroscopic nanocardboard plates has been observed. These plates are self-propelled through a photophoretic force from below, and thus exhibit this levitation without any moving parts. This is due to a near-continuum thermal creep across gaps in the plate. This paper presents a self-consistent model of photophoretic levitation for a disk. We analyse and combine the flows underneath the disk, and through cylindrical gaps in the disk surface, to generalise this levitation to higher Reynolds number flows and larger disks. We deduce that increasing the disk radius increases the levitation height, but the disk will not levitate under significant excess mass.

Introduction

Rarefied gas dynamics is concerned with gas flows where the mean free path λ is comparable to the characteristic length scale of the system L. We define the ratio of these terms to be the Knudsen number $Kn = \frac{\lambda}{L}$. In flow regimes where Kn is not negligible, the gas no longer moves as a continuum; that is, the Navier-Stokes equations that govern fluid flow - and the no-slip boundary condition that we use to solve them - start to break down. These rarefaction effects in a gas can be modelled by allowing a temperature gradient-dependent slip velocity at the boundary - a phenomenon called thermal creep [1]. In a recent experiment by Bargatin *et al.* [2] this was applied to create a self-levitating nanocardboard plate (fig. 1). This plate is heated by an LED from below, causing a temperature gradient across the height of the plate, inducing an airflow downward through gaps in the plate surface, which then propels the plate upwards (fig. 2). In this paper we model this airflow as a phenomenon caused by thermal creep.

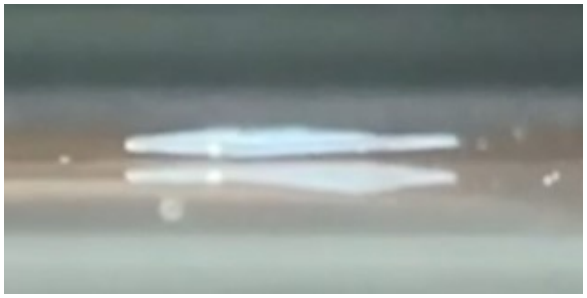

Figure 1: Photograph of the 0.5cm x 1cm levitating nanocardboard plate constructed by Bargatin [2].

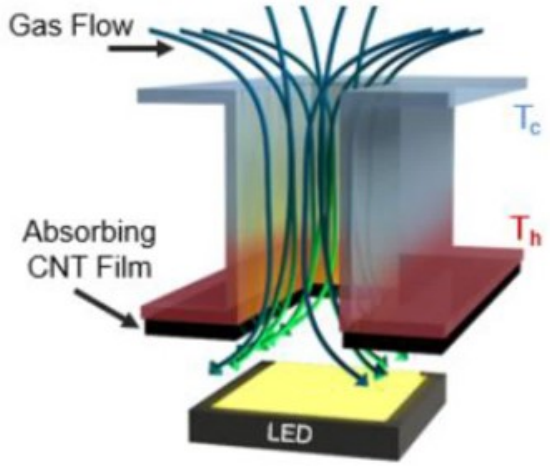

Figure 2: Diagram of Bargatin's apparatus used to levitate the plate [2]. This employs thermal creep-induced flow through gaps in the plate surface. Note the gas flow from the cold end to the hot end - a counter-intuitive result.

In this paper we model Bargatin's levitating plate as a disk, with cylindrical holes down its length representing the gaps, so as to create a self-consistent theory of levitating microdisks. For the flow underneath the disk, we replicate the analysis of Hinch [3] for disks floating above an air table,

with changed boundary conditions as elucidated in section 1. We then analyse the cylindrical gap flow induced by thermal creep in section 2, using theory derived from Nassios & Sader's paper [1] on asymptotic analysis of the Boltzmann equation. This incorporates our required near-continuum effects. We then combine these flows to develop a holistic picture of this levitation, deriving results for the levitation height in terms of different parameters. We see that levitation height increases as we increase the disk radius, but large temperature gradients are required to hold up significant payloads.

1 Flow Under the Disk

1.1 Governing Equations

We proceed with this analysis as per Hinch [3]. Let R_{disk} be the disk radius, p be the pressure and h be the levitation height. This flow is axisymmetric, so the velocity of air flow is (u, w) in cylindrical polar co-ordinates (r, z). The boundary conditions are

$$u = 0,\ w = 0,\ \text{when } z = 0,$$

$$u = 0,\ w = -q,\ \text{when } z = h,$$

$$p = p_a,\ \text{when } r = R_{\text{disk}},$$

where p_a is atmospheric pressure above the disk, and q is inflow velocity across the disk. Our continuity equation is

$$\frac{1}{r}\frac{\partial}{\partial r}(ru) + \frac{\partial w}{\partial z} = 0. \tag{1}$$

We introduce natural scaled variables for w, r and z:

$$\hat{w} = \frac{w}{q},\ \hat{r} = \frac{r}{R_{\text{disk}}},\ \zeta = \frac{z}{h},$$

which, when substituted into eq. (1), gives the scaled continuity equation

$$\frac{h}{qR_{\text{disk}}}\frac{1}{\hat{r}}\frac{\partial}{\partial \hat{r}}(\hat{r}u) + \frac{\partial \hat{w}}{\partial \zeta} = 0.$$

This gives us an appropriate scale for u:

$$\hat{u} = \frac{h}{qR_{\text{disk}}}u.$$

So, the scaled radial component of Navier-Stokes becomes

$$\hat{u}\frac{\partial \hat{u}}{\partial \hat{r}} + \hat{w}\frac{\partial \hat{u}}{\partial \zeta} = -\frac{h^2}{\rho R_{\text{disk}}^2 q^2}\frac{dp}{d\hat{r}} + \frac{\mu h}{\rho R_{\text{disk}}^2 q}\frac{1}{\hat{r}}\frac{\partial}{\partial \hat{r}}(\hat{r}\frac{\partial \hat{u}}{\partial \hat{r}}) - \frac{\mu h}{\rho R_{\text{disk}}^2 q}\frac{\hat{u}}{\hat{r}^2} + \frac{1}{Re}\frac{\partial^2 \hat{u}}{\partial \zeta^2},$$

where we define our Reynolds number for this flow under the disk to be

$$Re = \frac{\rho q h}{\mu}.$$

For thin gaps $h \ll R_{\text{disk}}$, we perform a regular perturbation expansion around infinetesimal $\frac{h}{R_{\text{disk}}}$, revealing that to leading order, the (unscaled) radial component of Navier-Stokes becomes

$$\rho(u\frac{\partial u}{\partial r} + w\frac{\partial u}{\partial z}) = -\frac{dp}{dr} + \mu\frac{\partial^2 u}{\partial z^2.} \tag{2}$$

Similarly, the z component reduces to

$$\frac{\partial p}{\partial z} = 0.$$

We need to find the pressure distribution under the disk $p(r)$. The force balance on the disk

$$Mg = \int \mathbf{n} \cdot \mathbf{T}\ dS = \int_0^{R_{\text{disk}}} 2\pi r(p - p_a)dr, \tag{3}$$

where $\mathbf{n}$ is the normal vector to the surface pointing into the fluid and $\mathbf{T}$ is the stress tensor, will then give the equation from which we can determine the levitation height.

1.2 Similarity Solution

There is a solution to this flow problem, namely the similarity solution for the boundary layer at an axisymmetric stagnation point. To permit this similarity solution in the thin gap, we ignore edge effects $O(\frac{h}{R_{\text{disk}}})$, so that

$$w = qf(\zeta)$$

for some function f, and $\zeta = \frac{z}{h}$ as defined in section 1.1. From axisymmetry, we may exploit the Stokes stream function

$$(u, w) = (-\frac{1}{r}\frac{\partial \Psi}{\partial z}, \frac{1}{r}\frac{\partial \Psi}{\partial r})$$

to give

$$u = -\frac{qr}{2h}f'(\zeta).$$

Substituting these velocity expressions into eq. (2) reduces it from a 2^{nd} order PDE to a 3^{rd} order ODE

$$-\frac{1}{2}f'^2 + ff'' - \frac{1}{Re}f''' = \frac{2h}{\rho r q^2}\frac{dp}{dr}, \tag{4}$$

with boundary conditions on f, rather than u and w:

$$f(0) = 0, f'(0) = 0, f(1) = -1, f'(1) = 0.$$

The LHS of eq. (4) only depends on ζ, and the RHS only depends on r, so we define our separation constant β such that

$$-2\beta = \frac{2h}{\rho r q^2}\frac{dp}{dr},$$

giving:

$$p = p_a + \frac{\rho q^2}{2h^2}(R_{\text{disk}}^2 - r^2)\beta, \tag{5}$$

$$-\frac{1}{2}f'^2 + ff'' - \frac{1}{Re}f''' = -2\beta. \tag{6}$$

Eq. (5) must be solved to find the pressure gradient coefficient β as a function of Re. We examine the limits of small and large Re, then combine these for an approximate (but asymptotically viable) solution for β.

1.3 Solution for $Re \ll 1$

We expand in a series for $Re \ll 1$, taking care to balance f terms with β terms. Such an expansion is:

$$f = f_0 + Re f_1 \text{ and } \beta = \frac{1}{Re}\beta_0 + \beta_1.$$

The leading order problem is

$$f_0''' = 2\beta_0 \text{ with } f_0(0) = 0, f_0'(0) = 0, f_0(1) = -1, f_0'(1) = 0,$$

which gives us

$$f_0 = 2\zeta^3 - 3\zeta^2 \text{ and } \beta_0 = 6.$$

Our first order problem is:

$$f_1''' = 2\beta_1 - \frac{1}{2}f_0'^2 + f_0 f_0'' \text{ with } f_1(0) = f_1'(0) = f_1(1) = f_1'(1) = 0,$$

which gives us

$$\beta_1 = \frac{27}{35}.$$

Bringing together our results for $Re \ll 1$, remembering we only need β for further analysis, we have found

$$\beta = \frac{6}{Re} + \frac{27}{35.}$$

1.4 Solution for $Re \gg 1$

For large Re, we use the method of dominant balance to find that a boundary layer of thickness $Re^{\frac{1}{2}}$ develops near the bottom surface at $\zeta = 0$, so as to permit the no-slip condition $f'(0) = 0$ there.

1.4.1 Outer Solution (Bulk Flow)

Outside the boundary layer, we expand

$$f = f_0 + Re^{-\frac{1}{2}} f_1 \text{ and } \beta = \beta_0 + Re^{-\frac{1}{2}} \beta_1,$$

so that the problem for the leading order is

$$-\frac{1}{2} f_0'^2 + f_0 f_0'' = -2\beta_0,$$

which satisfies all boundary conditions except the bottom slip condition:

$$f_0(0) = 0, \ f_0(1) = -1, \ f_0'(1) = 0.$$

This is satisfied by quadratics in ζ. Choosing the quadratic that satisfies these boundary conditions yields

$$f_0 = \zeta^2 - 2\zeta \text{ and } \beta_0 = 1.$$

This solution has a slip on the bottom surface $f_0'(0) = -2$.

1.4.2 Inner Solution (Boundary Layer)

We don't expand inside the boundary layer; rather, we define rescaled inner variables for velocity and height, so that we asymptotically balance velocity, as

$$F(\xi) = Re^{\frac{1}{2}} f(\zeta) \text{ with } \xi = Re^{\frac{1}{2}} \zeta.$$

So now, using $\beta = 1$ the governing equation (6) becomes:

$$-\frac{1}{2} F'^2 + FF'' - F''' = -2, \tag{7}$$

with boundary conditions

$$F(0) = 0 \text{ and } F'(0) = 0,$$

and matching condition

$$F' \to 2 \text{ as } \xi \to \infty.$$

Eq. (7) must be solved for numerically. Using a Runge-Kutta method, shooting from $\xi = 0$ and adjusting our guess for $F''(0)$ until $F' \to 2$, we find that

$$F \to -2\xi + 1.138 \text{ as } \xi \to \infty. \tag{8}$$

This is the outer part of our inner solution.

1.4.3 Matched Asymptotic Expansion

Rewriting eq. (8) in terms of the outer variable, we have

$$f \to -2\zeta + 1.138Re^{-\frac{1}{2}} \text{ as } \xi \to \infty.$$

We match this with the inner part of the outer solution (that is, the bulk flow solution at the bottom surface). For the bulk flow, our first order problem is:

$$-2\beta_1 = -f_0'f_1' + f_0f_1'' + f_1f_0'' = 2(1-\zeta)f_1' + \zeta(\zeta-2)f_1'' + 2f_1,$$

with boundary conditions

$$f_1(1) = 0,\ f_1'(1) = 0, \text{ and matching condition } f_1(0) = 1.138.$$

This is solved by

$$f_1 = 1.138(\zeta-1)^2 \text{ and } \beta_1 = 1.138.$$

Bringing together our results for $Re \gg 1$, we have found

$$\beta = 1 + 1.138Re^{-\frac{1}{2}}.$$

1.5 Final Calculations

We combine both asmyptotic results for our pressure gradient coefficient β to create an approximate solution for all Re, that has the correct asymptotic forms:

$$\beta = 1 + 1.138Re^{-\frac{1}{2}} + \frac{6}{Re}. \tag{9}$$

Finally, we combine eq. (5) with our force balance eq. (3) and β expression eq. (9) to get

$$Mg = \frac{\pi\rho q^2 R_{\text{disk}}^4\beta}{4h^2} = \frac{\pi\rho q^2 R_{\text{disk}}^4}{4h^2}(1 + 1.138\sqrt{\frac{\mu}{\rho q h}} + \frac{6\mu}{\rho q h}). \tag{10}$$

Note that eq. (10) implies that the photophoretic force goes as R_{disk}^4, which is promising for increasing the size of the system. Now, we must calculate the inflow velocity q, induced by thermal creep in the gaps, in order to create our self-consistent model and find the levitation height.

2 Flow in the Gaps

2.1 Results from Asymptotic Analysis of the Boltzmann Equation

In this subsection, we present the results derived by Nassios & Sader [1] for near-continuum flow, which we'll use to calculate the velocity through each gap. We restrict our analysis to the bulk flow,

as the inner flow in the Knudsen layer is negligible. We scale the variables as:

$$\tau = \frac{T}{T_0} - 1,$$

$$\mathbf{v} = \frac{\bar{\mathbf{v}}}{v_{\text{mp}}(T_0)},$$

$$\hat{r} = \frac{r_{\text{gap}}}{R_{\text{gap}}},$$

$$\hat{z} = \frac{z}{L},$$

$$P = \frac{R_{\text{gap}}^2}{\mu v_{\text{mp}}(T_0) L} p - 1,$$

$$k = \frac{\sqrt{\pi}}{2} Kn = \frac{\sqrt{\pi}}{2} \frac{\lambda}{2R_{\text{gap}}},$$

where τ is scaled temperature deviation from the equilibrium temperature T_0, $\bar{\mathbf{v}}$ is the average gas particle velocity and $\mathbf{v}$ is its scaled version, $v_{\text{mp}}(T_0)$ is the most probable collision speed at $T = T_0$, R_{gap} is the cylindrical gap radius and r_{gap} is the gap radius parameter (being careful to distinguish this from r, the disk radius parameter, which is important for when we combine these problems in section 3), λ is the mean free path of the gas, and k is the scaled Knudsen number. P is scaled pressure deviation, where we have obtained the scale by asymptotically balancing pressure with velocity in the Stokes equations, as per eq. (11) below. Note that we take our characteristic length to be the diameter of the gaps, because this is the minimum length scale in the gap flow.

Now, parameters $\mathbf{v}$, τ and P are expanded in k, such that

$$\alpha = \sum_{n=0} \alpha^{(n)} k^n$$

for the parameter α, where the superscript (n) gives the corresponding Knudsen order. In [1], Nassios & Sader derive the following governing equations for the bulk flow:

$$\begin{aligned} \nabla P^{(0)} &= \mathbf{0}, \\ \nabla \cdot \mathbf{v}^{(n)} &= 0, \\ \nabla P^{(n+1)} &= \nabla^2 \mathbf{v}^{(n)}, \\ \nabla^2 \tau^{(n)} &= 0. \end{aligned} \tag{11}$$

So, to each order in Knudsen number, we recover the Stokes equations for the bulk flow.

Nassios & Sader's Knudsen layer analysis gives the near-continuum corrections to flow problems as boundary conditions. To leading order, we have, at $\hat{r} = 1$:

$$\mathbf{v}^{(0)} = \mathbf{0},$$

which is no-slip, as expected. The first order gives, at $\hat{r} = 1$:

$$v_i^{(1)} t_i^{1,2} = k_0 S_{ij}^{(0)} n_i t_j^{1,2} + K_1 G_i^{(0)} t_i^{1,2},$$

$$v_i^{(1)} n_i = 0,$$

in the Einstein summation convention, where $t_i^{1,2}$ return the appropriate tangent vectors, n_i is the normal, k_0 and K_1 are Knudsen layer slip coefficients (derived in [1]), and we have defined $S_{ij}^{(n)}$ to be our rate of strain tensor, and $G_i^{(n)}$ to be our temperature gradient vector, where

$$S_{ij}^{(n)} = -(\frac{\partial v_i^{(n)}}{\partial x_j} + \frac{\partial v_j^{(n)}}{\partial x_i}), \text{ and } G_i^{(n)} = -\frac{\partial \tau^{(n)}}{\partial x_i}.$$

So we get a slip condition at $\hat{r} = 1$:

$$\mathbf{v} = (0, 0, -K_1 \frac{\partial \tau}{\partial \hat{z}}).$$

2.2 Calculation of Gap Velocity

Guided by the geometry of our system and form of our boundary conditions, our gap flow velocity is unidirectional, and circularly symmetrical. The continuity equation then gives us independence of z. So $\mathbf{v}^{(n)} = v^{(n)}(r)\hat{\mathbf{z}}$ and then eq. (11) reduces to:

$$\frac{\partial P}{\partial \hat{z}} = \frac{1}{\hat{r}} \frac{\partial}{\partial \hat{r}} (\hat{r} \frac{\partial v^{(n)}}{\partial \hat{r}}). \tag{12}$$

$R_{\text{gap}} \ll R_{\text{disk}}$, so pressure is constant over the gap entrance below the disk. Thus, we may assume pressure is independent of the gap radius parameter, despite depending on our disk radius parameter (as per eq. (5) in section 1). Our leading order boundary condition is just no-slip $v^{(0)}(\hat{r} = 1) = 0$, so solving eq. (12) gives us our leading order velocity

$$v^{(0)} = \frac{1}{4} \frac{\partial P}{\partial \hat{z}} (\hat{r}^2 - 1).$$

Our first order boundary condition is $v^{(1)}(\hat{r} = 1) = -K_1 \frac{\partial \tau}{\partial z}$, and so we get our first order solution for velocity:

$$v^{(1)} = \frac{1}{4} \frac{\partial P}{\partial \hat{z}} (\hat{r}^2 - 1) - K_1 \frac{\partial \tau}{\partial \hat{z}}.$$

So, all up, to first order,

$$v = v^{(0)} + kv^{(1)} = (1+k)\frac{1}{4}\frac{\partial P}{\partial \hat{z}}(\hat{r}^2 - 1) - kK_1\frac{\partial \tau}{\partial \hat{z}}. \tag{13}$$

We must unscale eq. (13) to combine it with the pressure eq. (5) and force balance eq. (3) from section 1. To simplify this expression, we first note that

$$\nu = \frac{\sqrt{\pi}}{4} v_{\text{mp}}(T_0)\lambda,$$

where ν is the kinematic viscosity $\frac{\mu}{\rho}$ at $T = T_0$. All up, unscaling gives:

$$\bar{v}_z = -\frac{2\nu K_1}{T_0}\frac{\partial T}{\partial z} + \frac{(1+k)(r_{\text{gap}}^2 - R_{\text{gap}}^2)}{4\mu}\frac{\partial p}{\partial z}, \tag{14}$$

which is the average gas particle velocity in the z-direction in each cylindrical gap.

3 Combining these Flows

In order to combine the flow under the disk with the flow inside the gaps, we must convert our gas velocity in the gap eq. (14) from section 2 to the constant inflow velocity q from section 1. First, we calculate the average velocity through the gap, so as to eliminate any dependence on r_{gap}:

$$v_{\text{av}} = \frac{1}{\pi R_{\text{gap}}^2}\int_{\text{gap}} \bar{v}_z \, dS = \frac{1}{\pi R_{\text{gap}}^2}\int_0^{2\pi}\int_0^{R_{\text{gap}}} \bar{v}_z r \, dr \, d\theta = -\frac{2\nu K_1}{T_0}\frac{\partial T}{\partial z} - \frac{(1+k)R_{\text{gap}}^2}{8\mu}\frac{\partial p}{\partial z}. \tag{15}$$

We note that our pressure gradient, temperature gradient, and K_1 are all negative, so we see that the temperature gradient is inducing a velocity down the gap into the reservoir, which is creating a pressure cushion in the reservoir, which drives a flow back up the gap, slightly decreasing its velocity.

We keep $\Delta T = T_0 - T_{\text{bottom}}$ as a variable parameter, where T_{bottom} is the temperature at the bottom of the disk. So, assuming both pressure and temperature vary linearly across the height of the disk, with atmospheric pressure p_a and equilibrium temperature T_0 at the top of the disk, eq. (15) becomes

$$v_{\text{av}} = -\frac{2\nu K_1}{T_0}\frac{\Delta T}{L} - \frac{(1+k)R_{\text{gap}}^2}{8\mu}\frac{\Delta p}{L},$$

which, when substituting in our expression for the pressure, eq. (5), gives:

$$v_{\text{av}} = -\frac{2\nu K_1}{T_0}\frac{\Delta T}{L} - \frac{(1+k)\beta q^2 R_{\text{gap}}^2(R_{\text{disk}}^2 - r^2)}{16\nu h^2 L}. \tag{16}$$

The back-flow caused by the pressure is small compared to the driving thermal creep term, so we retain downward flow through the gaps.

Now, to convert average gap velocity eq. (16) to a constant inflow velocity across the disk q, we make use of flow rate conservation; that is

$$Q_{\text{reservoir}} = Q_{\text{gaps}}$$

$$\implies \quad -q\pi R_{\text{disk}}^2 = \sum_{\text{gaps}} v_{\text{av}} \pi R_{\text{gap}}^2. \tag{17}$$

Subsituting eq. (16) and β from eq. (9) into eq. (17) gives us:

$$q = \frac{2N\nu K_1 \Delta T}{T_0 L}\left(\frac{R_{\text{gap}}}{R_{\text{disk}}}\right)^2 - \frac{(1+k)N\gamma R_{\text{gap}}^4}{16\nu h^2 L}\left(1 + 1.138\sqrt{\frac{\nu}{qh}} + \frac{6\nu}{qh}\right)q^2, \tag{18}$$

where N is our number of gaps, and

$$\gamma = \frac{1}{NR_{\text{disk}}^2}\sum_{\text{gaps}}(R_{\text{disk}}^2 - r^2)$$

is a dimensionless parameter that depends on our distribution of gaps across the disk surface, summing over all the radii values on the disk surface where we have a gap. This parameter could be changed to optimise our levitation height, as long as eq. (17) holds (that is, we have distribution of gaps across all of the disk radius). However, for our purposes, we assume equidistribution of gaps. A computer simulation gives $\gamma = \frac{1}{2}$ for such an equidistribution.

We may now combine eq. (18) with our force balance eq. (10) to solve for the levitation height.

4 Results

4.1 Comparison Between Theoretical Model and Existing Experiment

Rather than non-dimensionalising eq. (10) and eq. (18), we'll define our parameters to create a system of similar size to Bargatin's levitating plate in [2]. The geometry of Bargatin's plate gives 20% of the surface covered by gaps. Translating this to our disk problem, we have

$$N\pi R_{\text{gap}}^2 = \frac{\pi R_{\text{disk}}^2}{5}.$$

Bargatin also describes the ultralight material used, which gives a mass of $1g/m^2$. This gives

$$M = 0.8\ 10^{-3}\pi R_{\text{disk}}^2 + M_{\text{excess}},$$

where M_{excess} defines any additional payloads on top of the disk. The width of the gaps on Bargatin's plate is $25\mu m$, which is our characteristic length in the Knudsen number, so we must keep this identical, and thus we define $R_{gap} = 12.5\mu m$. The height of Bargatin's plate is $60\mu m$, so we'll define $L = 60\mu m$.

Nassios & Sader's paper [1] gives the value of the Knudsen slip coefficient $K_1 = -0.383$. Lastly, we'll define T_0 to be room temperature, and ν and ρ to be kinematic viscosity and density, respectively, at room temperature and atmospheric pressure. This produces the following system of equations from eq. (10) and eq. (18) for q and h in terms of ΔT, R_{disk}, and M_{excess}:

$$(0.8\ 10^{-3}\pi R_{\text{disk}}^2 + M_{\text{excess}})g = \frac{\pi\rho q^2 R_{\text{disk}}^4}{4h^2}(1 + 1.138\sqrt{\frac{\nu}{qh}} + \frac{6\nu}{qh}), \tag{19}$$

$$q = \frac{2\nu K_1 \Delta T}{5T_0 L} - \frac{(1+k)R_{\text{gap}}^2 R_{\text{disk}}^2}{160\nu h^2 L}(1 + 1.138\sqrt{\frac{\nu}{qh}} + \frac{6\nu}{qh})q^2. \tag{20}$$

We may now plot solutions for h against our 3 free parameters.

4.2 Levitation Height

Initially, we take our levitating disk with no payloads on top of it, so that $M_{\text{excess}} = 0$. In (fig. 3) we solve eq. (19) and eq. (20) simultaneously to plot levitation height against the temperature difference ΔT across the height of the disk for a few different radii; $R_0 = 0.5cm$ defines a system about the size of Bargatin's plate, while $100R_0 = 0.5m$ gives a disk of diameter $1m$, which is close to a life-sized hoverboard.

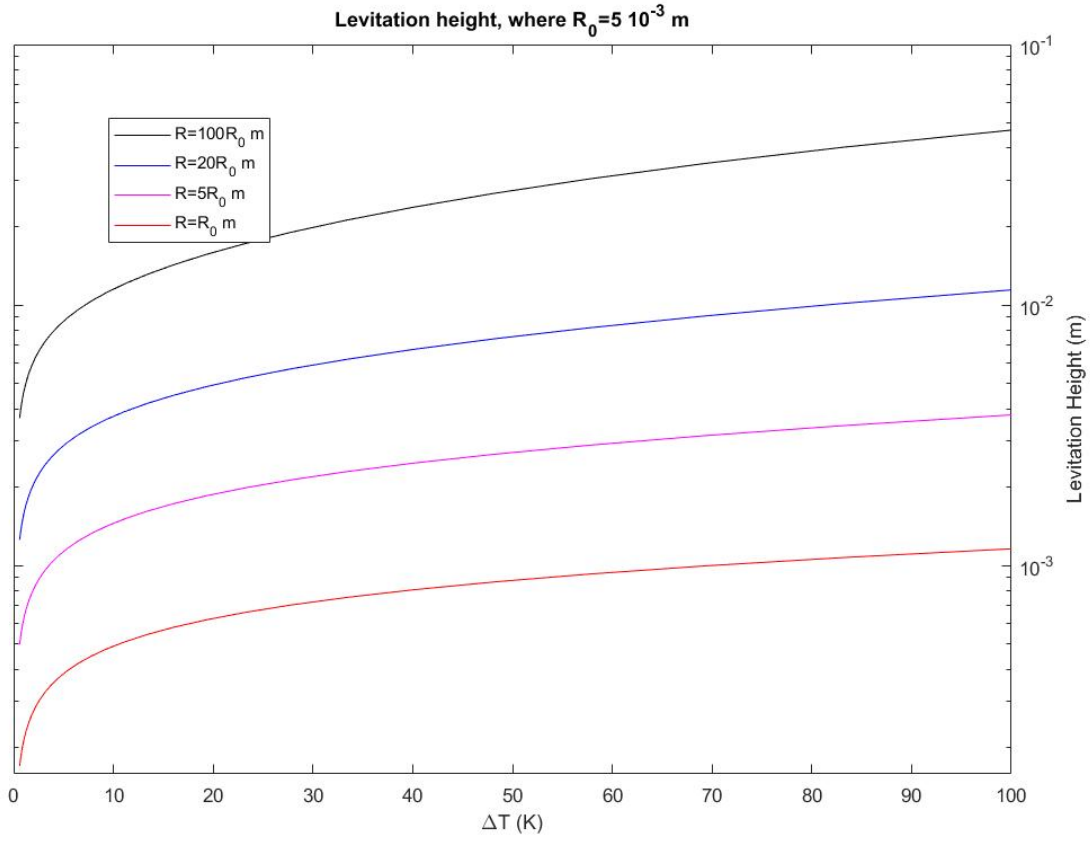

Figure 3: Plot of levitation height against temperature difference across the height of the disk, for various disk radii. R_0 gives a disk of similar area to the plate in Bargatin's experiment. $100R_0$ gives a disk of diameter $1m$. Note that levitation height is increasing as we increase the radius.

For the $1m$ diameter disk, with $\Delta T = 100K$, we get a levitation height of $h = 4.69cm$. In (fig. 4) we plot levitation height against excess mass for various temperature differences.

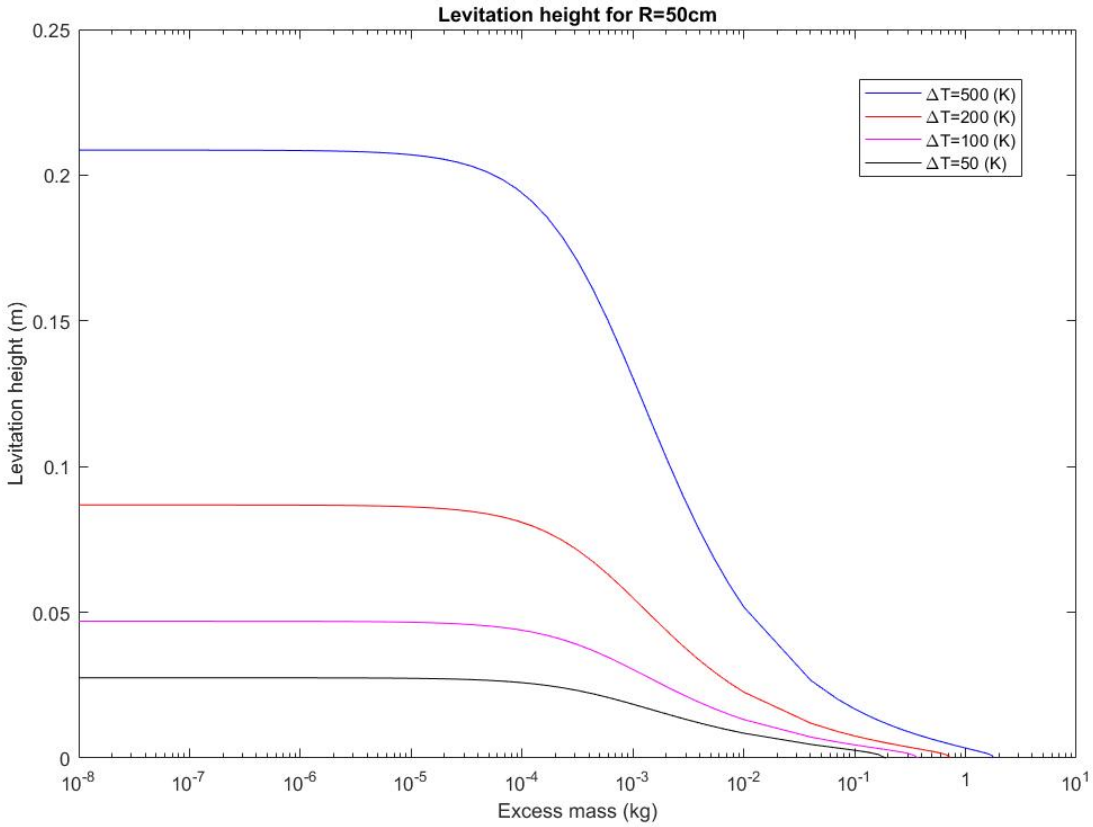

Figure 4: Plot of levitation height against excess mass for our $1m$ diameter disk, for various temperature differences across its height. We see that increasing the temperature difference increases levitation height and ability to take on additional payloads.

We see that with a temperature difference of $\Delta T = 500K$, the disk can hold up $M_{\text{excess}} = 1.79kg$ before touching the ground (levitation height $h = 0$).

These results, while exciting, do not take into account the structural integrity of the disk; a diameter of $1m$ with a height of $60\mu m$ is not sound. Future explorations into real-life applications of this research must take this into account, and thus increase the height with radius.

5 Conclusion

In this paper, we have created a self-consistent theory of photophoretic levitation. This theory models the observations of Bargatin's experiment on the levitation of nanocardboard plates [2], but by instead considering disks with cylindrical gaps. Bargatin's experiment describes an LED from below applying a temperature gradient across the height of the plate, inducing a photophoretic force on the bottom of the plate, holding the plate at some levitation height h above the ground. We model this phenomenon using the near-continuum theory of Nassios & Sader [1], considering the photophoretic force as caused by airflow through the gaps, which is induced by thermal creep. We replicate the analysis of Hinch [3] for disks floating on an air table, with different boundary conditions, combining this with our thermal creep flow to construct equations to solve for our levitation height. Our results show that increasing the radius of the disk will increase the levitation height, a promising result for scaling up the size of the system, provided that we maintain the percentage of surface area covered by gaps. The levitation height is also increased by increasing the temperature difference across the height of the disk. Both of these parameters increase the photophoretic force pushing the disk upward, and thus increase its capability to levitate under excess mass. This does not account for the structural instability of the disk when we keep the height constant, while increasing the radius, which will need to be considered for future applications. However, these results are fascinating and exciting, and open the door for potential applications at the macro scale, and for low and high Reynolds number flows.

References

1. Nassios, J & Sader J.E 2012, 'Asymptotic analysis of the Boltzmann–BGK equation for oscillatory flows', *Journal of Fluid Mechanics*, vol. 708, pp 197-249

2. Bargatin, I, *et al.* 2019, 'Photophoretic Levitation of Macroscopic Nanocardboard Plates', arXiv, 1910.03900

3. Hinch, E. J & Lemaitre, J 1994, 'The effect of viscosity on the height of disks floating above an air table', *Journal of Fluid Mechanics*, vol. 213, pp. 313-322